

COMMUNICATION

Cooperative Omega Loops in Cytochrome *c*: Role in Folding and Function

Mallela M. G. Krishna*, Yan Lin, Jon N. Rumbley and S. Walter Englander

Department of Biochemistry
and Biophysics, Johnson
Research Foundation
University of Pennsylvania
School of Medicine, 422 Curie
Blvd, 1007 Stellar Chance Bldg
Philadelphia, PA 19104-6059
USA

Hydrogen exchange experiments under slow exchange conditions show that an omega loop in cytochrome *c* (residues 40–57) acts as a cooperative unfolding/refolding unit under native conditions. This unit behavior accounts for an initial step on the unfolding pathway, a final step in refolding, and a number of other structural, functional and evolutionary properties.

© 2003 Elsevier Ltd. All rights reserved

*Corresponding author

Keywords: omega loop; protein folding; hydrogen exchange; cytochrome *c*; protein function

Leszczynski and Rose found that a category of non-regular protein secondary structure, which they called the Ω loop, accounts for 25% of the amino acid residues in protein molecules.¹ The termini of Ω loops come close in three-dimensional space and their side-chain atoms pack tightly but irregularly to produce compact substructures. Ω loops tend to occur at the protein surface and serve important functional roles.^{1,2} Results described here and in related papers^{3–6} contribute to this view by identifying Ω loops in cytochrome *c* (Cyt *c*) as cooperative units that participate in a number of functional activities, including the step-wise Cyt *c* folding/unfolding pathway.

Thermodynamic principles require that proteins must constantly unfold and refold, even under native conditions. All of the molecules cycle through all possible higher energy partially and fully unfolded forms, albeit at a very low level. Most observational methods are dominated by signals from the overwhelmingly populated native state and so are insensitive to this transient unfolding behavior. In contrast, the hydrogen exchange (HX) rates of structurally protected hydrogen atoms receive no contribution from the static native

state. Under favorable conditions, the otherwise invisible low level unfolding reactions can be made to dominate the HX behavior of the amino acids that they expose. HX results can then identify the major higher energy states and measure their equilibrium^{4,5} and kinetic⁶ parameters.

Previous HX experiments found four concerted unfolding units (foldons) in Cyt *c*, illustrated in Figure 1(a).^{4–8} Some of these are coincident with entire helices, consistent with their intrinsically cooperative nature.^{9,10} Previous results suggested that Ω loops could also behave as concerted folding units but this was not well documented due to the small number of amide protons measured. Experiments described here, done under more favorable conditions, reveal a new foldon, an entire Ω loop, that was not detected in earlier work (Figure 1). This foldon accounts for a concerted step on the Cyt *c* folding pathway. It also serves a number of other functional purposes.

Concerted unfolding of an Ω -loop

The ability of HX experiments to identify a cooperative folding unit depends critically on the number of exchanging hydrogen atoms that can be measured. To maximize this number, the present work used the more stable reduced form of Cyt *c* at lower temperature (20 °C) than before and at a series of lower pH values. Figure 2 shows the pH dependence for exchange of the measurable amide protons in the four previously characterized foldons. The conditions used increase the number of measurable protons in the Yellow loop to 17,

Abbreviations used: Cyt, *c*, cytochrome *c*; WT, wild-type; pWT, pseudo wild-type (H26N, H33N); HX, hydrogen exchange; NHX, native state hydrogen exchange; PUF, partially unfolded form; foldon, cooperative folding/unfolding unit; GdmCl, guanidinium chloride.

E-mail address of the corresponding author: mmg@hx2.med.upenn.edu

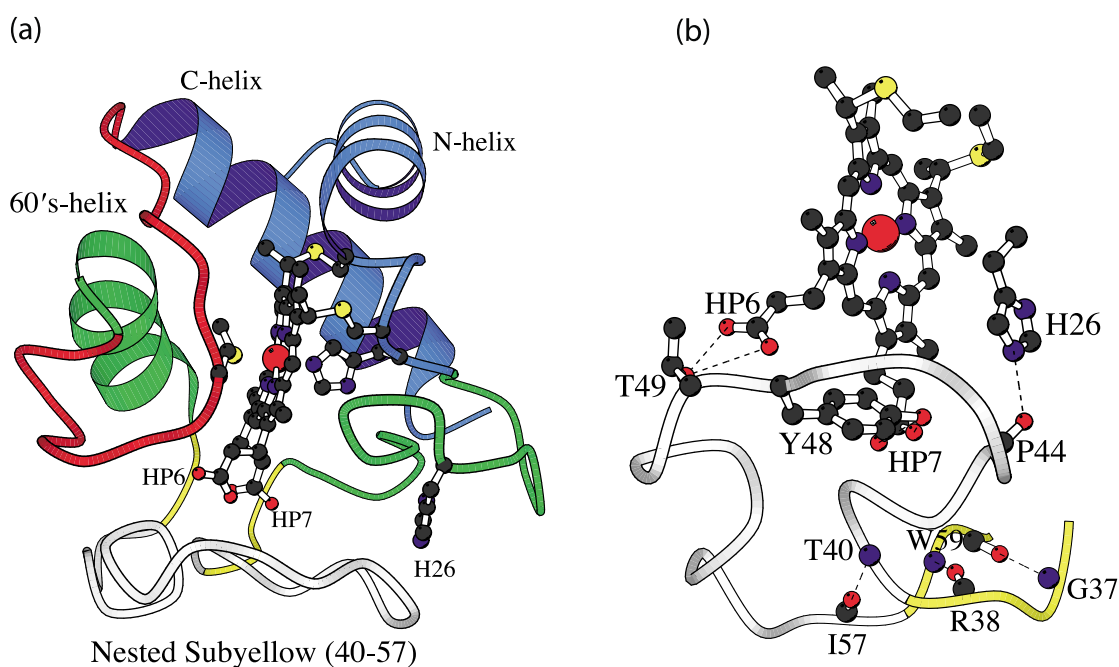


Figure 1. Molecular Cyt *c* structure (1HRC.pdb¹³ and MOLSCRIPT³⁸). (a) The five foldons are the Red unit (71–85 Ω loop), the outer Yellow neck (a short anti-parallel β -sheet; residues 37–39, 58–61), the N-yellow Ω loop (residues 40–57), the Green unit (60's helix and 20's–30's Ω -loop), and the Blue unit (N and C-terminal helices).^{4,7,8} The outer Yellow neck and the N-yellow Ω loop constitute the previously characterized Yellow unit (residues 37–61).^{4,7,8} (b) The N-yellow Ω loop viewed from below showing the pH-sensitive hydrogen bonds to His26 (with Pro44 CO) and other interactions.

compared to four in oxidized Cyt *c*⁴ and six in reduced Cyt *c*⁸ when measured at p²H 7 and 30 °C. A similar increase was obtained for the Red loop but not for the Green loop.

Most of these hydrogen atoms exchange by way of small “local fluctuations” that expose to exchange only one protected hydrogen at a time.^{11,12} Hydrogen atoms may also exchange by way of larger unfolding reactions but this behavior is often obscured by faster exchange through local fluctuation pathways. Previous native state hydrogen exchange (NHX) experiments exploited denaturant, temperature, or pressure to selectively promote the large concerted unfolding reactions so that they come to dominate the exchange of the hydrogen atoms that they expose. The otherwise hidden large unfolding reactions are then revealed by the merging of the multiple hydrogen atoms exposed by each unfolding to a common HX rate (EX1 exchange)⁶ or to a common equilibrium ΔG_{HX} (EX2 exchange).^{4,5}

Figure 2 shows that low pH selectively promotes an otherwise hidden large unfolding reaction that exposes a subset of nine measurable amide protons to solvent exchange. They are placed sequentially within the Yellow loop segment (Thr40, Gln42, Ala43, Phe46, Asn52, Lys53, Asn54, Lys55, Ile57). (The missing hydrogen atoms exchange too fast to measure.) Only one of these, Gln42, was observed in earlier work.⁸ The other amide protons near the termini of the previously studied Yellow loop and in the other foldons do not join this trend.

Figure 3(a) and (b) exhibit these nine hydrogen atoms alone at different salt conditions. Figure 3(c) shows that increasing denaturant tends to cause similar merging, as for other cooperative foldons found before.

The concerted 40–57 segment is an ideal Ω loop (Figure 1(b)) nested within the larger cooperative unit previously referred to as the Yellow loop (residues 37–61). The terminal residues are hydrogen bonded (40NH–57CO) and there are a large number, 32, of intra-loop residue-residue contacts. The HX results identify this loop as a separate cooperative unfolding unit. We refer to it as the Nested yellow (N-yellow) foldon. It corresponds well with one of the Ω loops (40–54) found by the original analysis by Leszczynski and Rose.¹ The outer neck of the loop, a small anti-parallel β -sheet,¹³ unfolds reversibly with higher free energy.

Selective unfolding at low pH

Figure 3(a) and (b) show that the pH-dependent merging of the N-yellow protons has little dependence on salt concentration, indicating that the loop destabilization is not due to general electrostatic repulsion. In fact, high salt modestly promotes rather than retards the merging. The concerted N-yellow unfolding must be promoted by one or more buried titratable groups that have protonation pK_a more favorable in the unfolded than

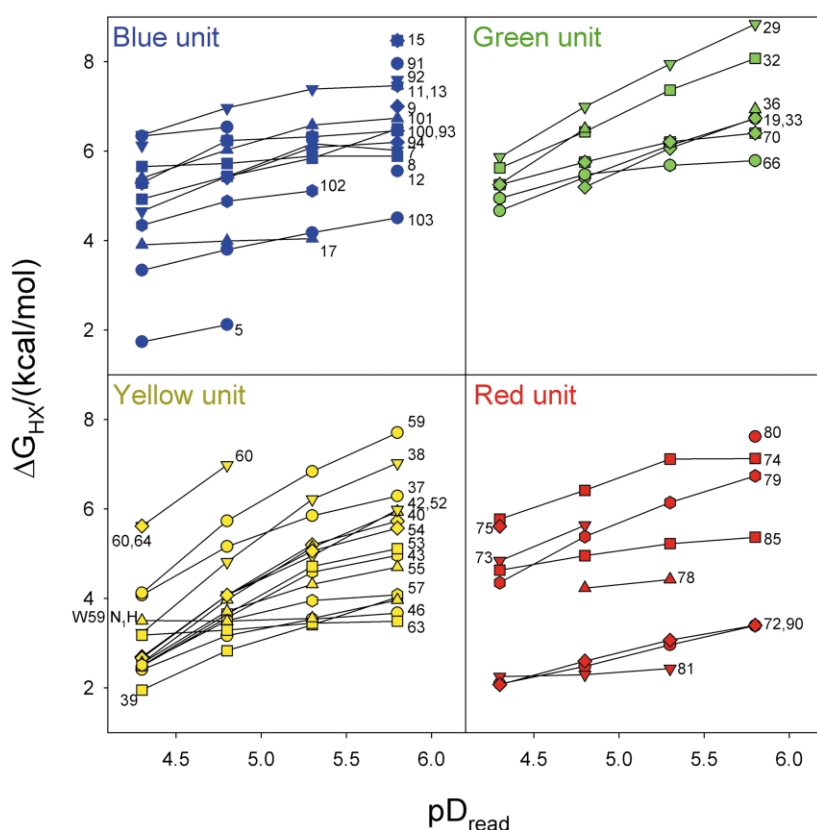


Figure 2. NHX of reduced Cyt *c* showing the selective promotion of a large unfolding reaction at low p²H (20 °C with 0.5 M KCl). Measured H to ²H exchange rates, k_{ex} , were converted to the free energy of the responsible structural opening reaction using the equation $\Delta G_{\text{HX}} = -RT \ln(k_{\text{ex}}/k_{\text{ch}})$, which holds in the EX2 region below pH ~ 10. Here, k_{ch} is the chemical exchange rate calculated for unprotected amides.^{39,40} Errors in reported ΔG_{HX} values are generally less than 0.1 kcal/mol. The amide protons are color-coded according to the previously characterized four foldons^{4,7,8} (Figure 1). HX rates are slowed at lower pH due to the dependence of the chemical exchange rate on OH ion. In addition some of the ΔG_{HX} values show a general decrease with low pH, perhaps due to the large build-up of positive charge, but they become pH-independent above p²H 6. Equine Cyt *c* (type VI) from Sigma Chemicals was used in these experiments. The purity was checked and it was further purified by reverse phase HPLC when necessary.¹⁵ All other chemicals

were as described.^{4,7,8} The pH buffers used were 0.1 M phosphate, succinate, citrate, acetate, and formate. All experiments were done at 20 °C in the presence of 0.5 M KCl. NHX was initiated by passing reduced Cyt *c* (ascorbate) in H₂O buffer through a Sephadex G25 spin column previously washed with H₂O/dithionite and then equilibrated with deoxygenated ²H₂O buffer (argon bubbling, 40 mM ascorbate). The sample was transferred to an NMR tube, filled with argon, and capped. Time-points were collected for ten days. NMR parameters and data analysis were as described.^{4,7,8} Typical protein concentration was ~6 mM. The dead-time from the start of the HX reaction was ~15 minutes.

in the folded form due to bonding interactions that are lost on unfolding.

Buried protonatable groups linked to the N-yellow segment are His26 and the heme propionates (Figure 1(b)). The pK_a for protonation of His26 is less than 3.6 in the native state¹⁴ compared to ~6.5 for an exposed histidine. One of the two heme propionates, probably heme propionate 7, has a pK_a for protonation less than 4.5 compared to 5–6 in water.¹⁴ We did NHX experiments with a mutant lacking His26 (H26N, H33N), called pseudo-wild-type (pWT) Cyt *c*.¹⁵ The ΔG_{HX} values of the N-yellow protons still merge but only at more extreme pH (Figure 3(d)). Similar results were obtained at various salt concentrations (not shown). These results indicate that His26 does contribute to the selective pH sensitivity of the N-yellow unfolding but some other group is also necessary, presumably the heme propionate.

Extrapolation of the data in Figure 3(a) and (b) to $\Delta G_{\text{HX}} \sim 0$ shows that the pH-driven equilibrium transition of the N-yellow loop is essentially coincident with the low pH molten globule transition of

Cyt *c*. Further, the N-yellow transition matches the surprising result that high salt promotes rather than shields against the Cyt *c* molten globule transition.¹⁶ These results suggest that the special ability of low pH to produce the partially unfolded molten globule form of Cyt *c*, and other proteins also, might be explained by the selective destabilization and unfolding of particular foldons. Other destabilants (denaturant, temperature, pressure) affect foldons in a different way as shown by previous NHX experiments and will not in general produce a molten globule.

Ω Loops act as cooperative folding units

In previous NHX work, six residues distributed through the Red Ω loop of Cyt *c* (15 residues total) were found to exhibit the same equilibrium and kinetic parameters for reversible unfolding (ΔG_{HX} , k_{op} , k_{cl}), showing that the entire Red loop acts as a cooperative unfolding/refolding unit.⁶ The unit unfolding of the large Yellow Ω loop was inferred before from the common ΔG_{HX} measured for three amides and the Trp59 indole N₁H in the outer

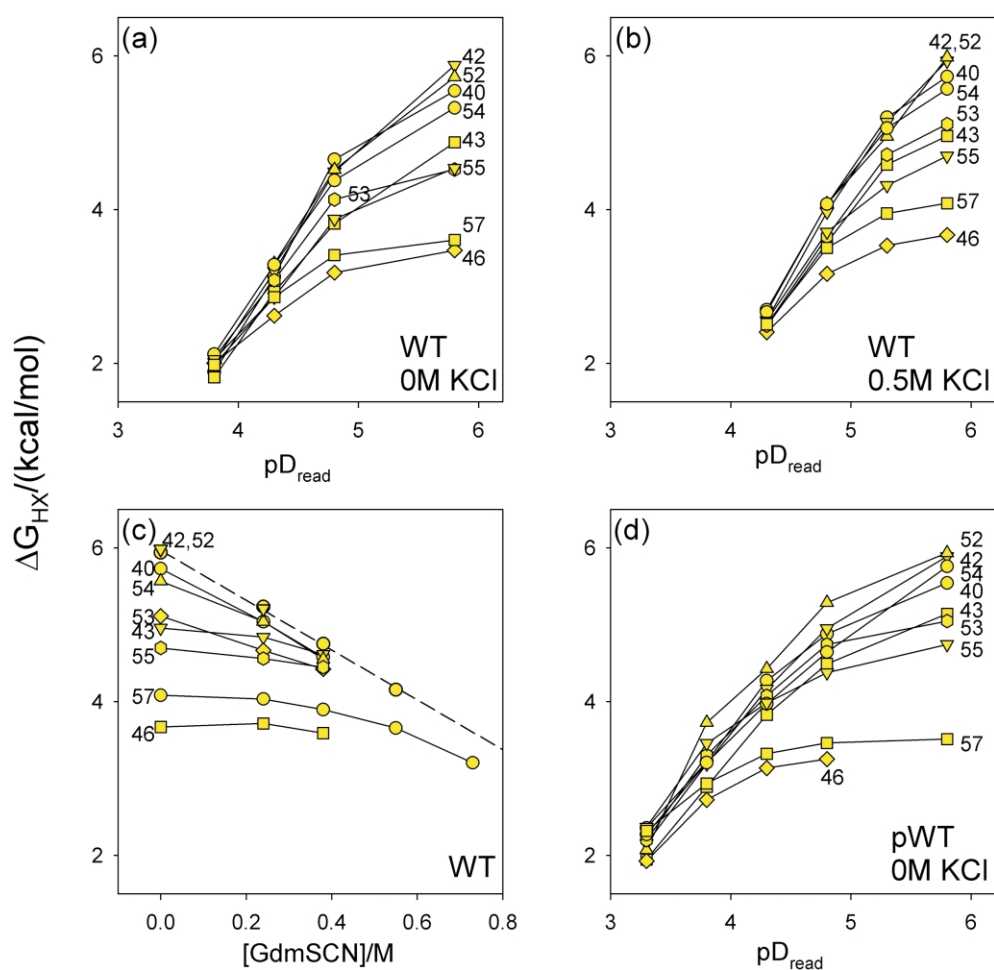


Figure 3. NHX of the N-yellow loop hydrogen atoms in reduced Cyt *c*. (a) and (b) The independence of ΔG_{HX} on salt concentration for WT Cyt *c* (similar results for intermediate salt concentrations and for higher pH not shown). (c) The dependence on denaturant (GdmSCN at p^2H_{read} 5.8). Measurements become difficult at higher denaturant concentrations due to faster rates and decreasing NMR peak amplitudes. The broken line shows the straight line fit to the marker protons, Gln42 and Asn52. (d) pH-dependent merging is slower for pWT Cyt *c* (H26N, H33N), indicating a role for His26, but some similar merging behavior continues, indicating a role for an additional buried group, apparently heme propionate. Experimental conditions were as described in the legend to Figure 2.

Yellow neck.^{4,7,8} The present results show that the included N-yellow loop reversibly unfolds as a separate unit. The outer Yellow neck residues unfold at higher free energy, producing a partially unfolded state that includes the unfolded N-yellow and Red loops.

The present results indicate that the N-yellow foldon unfolds with free energy of 5.0 kcal/mol above the native state in oxidized Cyt *c* and 6.7 kcal/mol in the reduced state. Previous results show that the concerted Red loop has unfolding free energy of 6.0 kcal/mol and 9.2 kcal/mol in oxidized and reduced Cyt *c*.⁴⁻⁸ The outer Yellow neck unfolds with a free energy of 7.4 kcal/mol and 10.6 kcal/mol in oxidized and reduced Cyt *c*. All of these values refer to p^2H 7.0 at 20 °C.

These results characterize the concerted unfolding of three Ω loops. Concerted unfolding appears to be a common Ω loop property.

Foldon relationships

At low pH where the concerted N-yellow unfolding comes to dominate the exchange of all of its protons, the protons protected in other foldons exchange more slowly (Figure 2). They are not exposed to exchange in the N-yellow unfolding. The same result is seen up to neutral pH in Figure 4(a), which compares marker protons for the N-yellow, Red, outer Yellow, and Green helix foldons. (Marker protons exchange only by way of the large unit unfolding reactions.) These results indicate that the N-yellow Ω loop unfolds independently of (before) the other unfoldings.

That the N-yellow foldon unfolds before the others is also indicated by a direct measurement of the unfolding rates of the different foldons by a kinetic NHX (kNHX) method, which measures reversible unfolding by HX under EX1 conditions. Figure 4(b) shows some kNHX results for

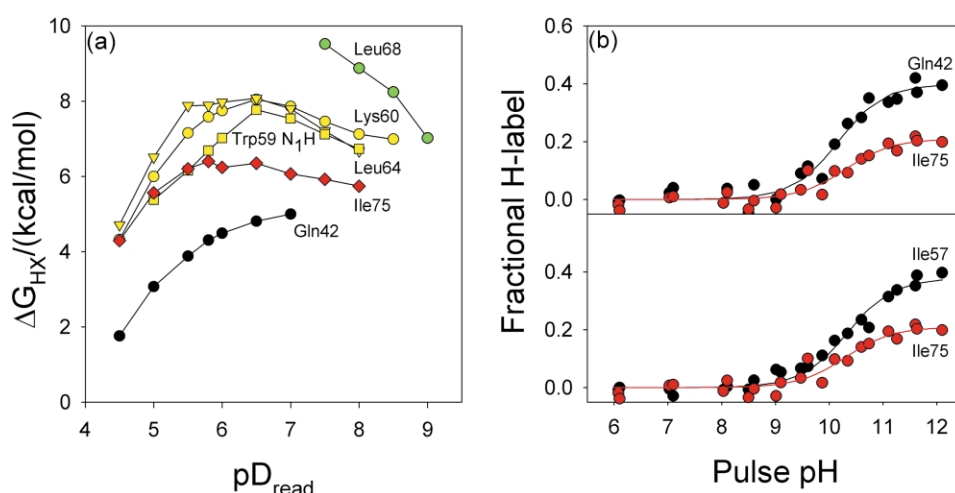


Figure 4. Unfolding equilibria and rates (oxidized Cyt *c*). (a) The dependence of foldon stability on p^2H , measured by marker protons for the N-yellow (Gln42), Red (Ile75), outer Yellow (Lys60, Leu64, Trp59 indole N₁H), and Green (Leu68) foldons. The NHX experiments were done as described.⁴ (b) Kinetic NHX results for marker protons of the N-yellow and Red foldons in oxidized Cyt *c*. The plateau at high pH shows EX1 exchange where HX rate equals the (reversible) unfolding rate. In these experiments, done as described by Hoang *et al.*,⁶ native Cyt *c* was exposed to 2H to H exchange at high pH for only a short time (33 ms), then analyzed for H-labeling levels by NMR at p^2H_{read} 5.3.

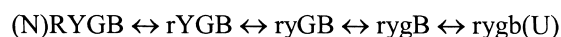
marker protons in the N-yellow and Red loops. In these experiments, oxidized Cyt *c* was exposed to a short pulse of H- 2H exchange labeling (33 ms) at increasing pH. At relatively low pH, where structural reclosing is faster than exchange ($k_{cl} > k_{ch}$; $k_{ex} = K_{op}k_{ch}$), the reversible unfolding reaction acts as a pre-equilibrium step (EX2 region). HX rate increases with pH (OH-ion catalyzed) until it limits at the dynamic reversible unfolding rate (EX1 limit; $k_{cl} < k_{ch}$; $k_{ex} = k_{op}$). The unfolding rate is sensitively indicated by the pH-independent plateau level of labeling reached at high pH.⁶ The unfolding rate is $16(\pm 1) s^{-1}$ for the N-yellow unit and $7(\pm 1) s^{-1}$ for the Red unit. Thus the N-yellow Ω loop opens first.

The kNHX data in Figure 4(b) also yield a ΔG_{HX} value for N-yellow unfolding in the EX2 region between pH 9 and 11. It is the same as at neutral pH (Figure 4(a)), but all of the higher free energy foldons are destabilized by ~ 2 kcal/mol.⁶ This behavior is due to a buried titratable group that can be deprotonated at high pH when the transient N-yellow unfolding exposes it to attack by some incoming solvent base (first step in the Cyt *c* alkaline transition; see the accompanying paper³). The buried negative charge then promotes the unfolding of the Red loop and of the higher lying unfoldings but not of the lower lying N-yellow loop.

These equilibrium and kinetic observations indicate that the N-yellow Ω loop unfolds before the other foldons. However the other foldons are not independent of N-yellow. The marker protons in Figure 4(a) show that the selective destabilization of the N-yellow unfolding at low pH is mirrored in the behavior of the higher lying Red and Yellow foldons. This indicates that N-yellow loop unfolding is included within the Red and Yellow loop unfoldings, consistent with a sequence in which N-yellow unfolds first, as in reaction Scheme 2 below.

Functional correlations: the folding pathway

Previous experiments showed that the Red, Yellow, Green, and Blue foldons in Cyt *c* do not simply unfold independently. They unfold in an interdependent, sequential way that constructs an unfolding pathway, as in reaction Scheme 1 (foldons color-coded; native fold in upper case, unfolded in lower case). The evidence for this important result can be briefly summarized. In Cyt *c*, the order of increasing unfolding size (m value) and unfolding free energy for the different foldons was found to be Red open, Yellow open, Green open, Blue open.^{4,5,8} In agreement, a stability labeling experiment⁷ identified the partially unfolded forms (PUFs) as follows: Red alone unfolded (rYGB), Red + Yellow unfolded (ryGB), Red + Yellow + Green unfolded (rygB), and finally all unfolded (rygb) to produce the U state. The identity of these PUFs differ, one from another, by one foldon and they are just the forms necessary to construct the sequential unfolding pathway in Scheme 1. kNHX experiments find that the temporal order of unfolding is in this same sequence.⁶ Other results independently demonstrate that rYGB and rygB are on the folding/unfolding pathway, and place them as shown in Scheme 1.^{6,17,18}



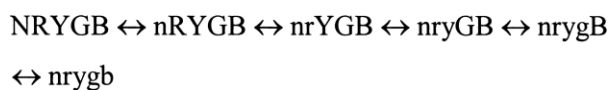
Scheme 1.

These prior experiments⁴⁻⁸ were done under equilibrium native conditions where the native state is by far the most abundant form. The results identify, and define the kinetic sequence of,

transient reversible unfolding steps that occur continually at a very low level at equilibrium ($K_{op} < 10^{-2}$). Because the system is at equilibrium, each unfolding step found by the HX experiments must be matched by an equal and opposite refolding reaction. Therefore the major refolding pathway found in this way must replicate the major unfolding pathway, as in [Scheme 1](#). NHX results for other proteins^{19–22} support the generality of this kind of folding/unfolding behavior.

It is revealing that the experimentally derived folding sequence conforms to the structure of native Cyt *c* ([Figure 1\(a\)](#) and Rumbley *et al.*²³). The Blue unit contacts only the Green unit, therefore initial folding of the Blue bihelical unit forms a docking surface that can template the formation of and stabilize only the Green unit. In turn the Green unit is necessary to guide and stabilize the formation of the Yellow and Red units.²³ This correspondence between the native structure and the independently derived pathway strongly suggests that folding proceeds in the native context, and is determined by native-like interactions, with prior units of native-like structure guiding and stabilizing the formation of subsequent units in a stepwise assembly process.

The present experiments were similarly done at equilibrium native conditions. The results reveal a previously unrecognized foldon, the N-yellow unit, and show that the N-yellow loop unfolds faster and at lower free energy than the other foldons, i.e. it can unfold alone (nRYGB). It further appears that the higher lying Red-unfolded and Yellow-unfolded forms include the N-yellow loop (nrYGB and nryGB, respectively; [Figure 4\(a\)](#) and [\(b\)](#)). These results are consistent with reaction [Scheme 2](#). Another possibility, not wholly ruled out by available data, is that the N-yellow and Red units may unfold as alternative initial steps, and then join to form nrYGB.



Scheme 2.

Other functional correlations

The nested yellow foldon, which is the least stable and fastest unfolding unit, is involved in a remarkable number of structural, functional and evolutionary features of Cyt *c*.

In regard to structural dynamics, different proteases cleave Cyt *c* first within the N-yellow loop^{24,25} suggesting that it is the most flexible unit. From their protease studies, Wang & Kallenbach²⁴ calculate a redox-dependent free energy difference of 2 kcal/mol, close to the 1.7 kcal/mol found here for N-yellow unfolding. This is consistent with the

view that protease accessibility is determined by the transient unfolding,²⁶ which is more favorable in oxidized than in reduced Cyt *c*. Decreased N-yellow loop stability of some recombinant Cyt *c* variants correlates with decreased expression levels, suggesting increased intracellular proteolysis rates^{27,28} (J.N.R., unpublished results). Molecular dynamics simulations²⁹ and ¹⁵N relaxation measurements^{30,31} also indicate that the N-yellow loop is more dynamic than the other units.

In functional interactions, the N-yellow loop unfolds: (1) as a first step in Cyt *c*-mediated apoptosis and necrosis;³² (2) when Cyt *c* binds to lipid membranes;³² (3) as a first step in the alkaline transition.^{3,32} When the N-yellow loop is destabilized or even removed, Cyt *c* maintains the same overall fold and its characteristic heme absorption bands.^{33–35} However, its activity, redox potential, and ability to bind to its redox partners decrease and the alkaline transition is promoted.^{28,33,34,36}

The N-yellow loop is the least conserved in Cyt *c* evolution. It is deleted as a unit in some proteins, e.g. *Pseudomonas* Cyt *c* and dimers like Cyt *c*₄.³⁷ Class I cytochromes are categorized based on whether or not the N-yellow loop is present.³⁷

Conclusions and implications

The results presented here indicate that Ω loops in globular proteins continually unfold and refold as concerted units under native conditions. These and other results show that the globular Cyt *c* protein is composed of five foldon units and imply that the folding behavior of Cyt *c* emerges as an epiphenomenon of its foldon substructure. The stepwise nature of the folding pathway is determined by the unit cooperative nature of the individual foldons; the pathway sequence is determined by the organization of the foldons within the native structure.

The N-yellow loop, the least stable foldon in Cyt *c*, accounts for the first step in the unfolding pathway and it participates importantly in other functional activities. The accompanying paper³ identifies another functional role of the N-yellow and Red Ω loop foldons. These results raise the interesting possibility that the foldon substructure of proteins may determine not only their folding behavior but also additional functional properties.

Acknowledgements

This work was supported by research grants from the NIH and the Mathers Foundation.

References

1. Leszczynski, J. F. & Rose, G. D. (1986). Loops in

- globular proteins: a novel category of secondary structure. *Science*, **234**, 849–855.
2. Fetrow, J. S. (1995). Omega loops: nonregular secondary structures significant in protein function and stability. *FASEB J.* **9**, 708–717.
 3. Hoang, L., Maity, H., Krishna, M. M. G., Lin, Y. & Englander, S.W. (2003). Folding units of cytochrome *c* govern its alkaline transition. *J. Mol. Biol.* **331**, 37–43.
 4. Bai, Y., Sosnick, T. R., Mayne, L. & Englander, S. W. (1995). Protein folding intermediates: native-state hydrogen exchange. *Science*, **269**, 192–197.
 5. Bai, Y. & Englander, S. W. (1996). Future directions in folding: the multi-state nature of protein structure. *Proteins: Struct. Funct. Genet.* **24**, 145–151.
 6. Hoang, L., Bedard, S., Krishna, M. M. G., Lin, Y. & Englander, S. W. (2002). Cytochrome *c* folding pathway: kinetic native-state hydrogen exchange. *Proc. Natl Acad. Sci. USA*, **99**, 12173–12178.
 7. Xu, Y., Mayne, L. & Englander, S. W. (1998). Evidence for an unfolding and refolding pathway in cytochrome *c*. *Nature Struct. Biol.* **5**, 774–778.
 8. Milne, J. S., Xu, Y., Mayne, L. C. & Englander, S. W. (1999). Experimental study of the protein folding landscape: unfolding reactions in cytochrome *c*. *J. Mol. Biol.* **290**, 811–822.
 9. Zimm, G. H. & Bragg, J. K. (1959). Theory of the phase transition between helix and random coil in polypeptide chains. *J. Chem. Phys.* **31**, 526–535.
 10. Lifson, S. & Roig, A. (1961). On the theory of the helix-coil transition in polypeptides. *J. Chem. Phys.* **34**, 1963–1974.
 11. Milne, J. S., Mayne, L., Roder, H., Wand, A. J. & Englander, S. W. (1998). Determinants of protein hydrogen exchange studied in equine cytochrome *c*. *Protein Sci.* **7**, 739–745.
 12. Maity, H., Lim, W. K., Rumbley, J. N. & Englander, S. W. (2003). Protein hydrogen exchange mechanism: local fluctuations. *Protein Sci.* **12**, 153–160.
 13. Bushnell, G. W., Louie, G. V. & Brayer, G. D. (1990). High-resolution three-dimensional structure of horse heart cytochrome *c*. *J. Mol. Biol.* **214**, 585–595.
 14. Moore, G. R. & Pettigrew, G. W. (1990). *Cytochromes c: Evolutionary, Structural and Physicochemical Aspects*. Springer Series in Molecular Biology, Springer-Verlag, Berlin, Heidelberg, New York.
 15. Rumbley, J. N., Hoang, L. & Englander, S. W. (2002). Recombinant equine cytochrome *c* in *Escherichia coli*: high-level expression, characterization, and folding and assembly mutants. *Biochemistry*, **41**, 13894–13901.
 16. Goto, Y., Hagihara, Y., Hamada, D., Hoshino, M. & Nishii, I. (1993). Acid-induced unfolding and refolding transitions of cytochrome *c*: a three-state mechanism in H₂O and D₂O. *Biochemistry*, **32**, 11878–11885.
 17. Roder, H., Elove, G. A. & Englander, S. W. (1988). Structural characterization of folding intermediates in cytochrome *c* by H-exchange labeling and proton NMR. *Nature*, **335**, 700–704.
 18. Bai, Y. (1999). Kinetic evidence for an on-pathway intermediate in the folding of cytochrome *c*. *Proc. Natl Acad. Sci. USA*, **96**, 477–480.
 19. Englander, S. W. (2000). Protein folding intermediates and pathways studied by hydrogen exchange. *Annu. Rev. Biophys. Biomol. Struct.* **29**, 213–238.
 20. Chamberlain, A. K. & Marqusee, S. (2000). Comparison of equilibrium and kinetic approaches for determining protein folding mechanisms. *Advan. Protein Chem.* **53**, 283–328.
 21. Yan, S., Kennedy, S. D. & Koide, S. (2002). Thermodynamic and kinetic exploration of the energy landscape of *Borrelia burgdorferi* OspA by native-state hydrogen exchange. *J. Mol. Biol.* **323**, 363–375.
 22. Chu, R., Pei, W., Takei, J. & Bai, Y. (2002). Relationship between the native-state hydrogen exchange and folding pathways of a four-helix bundle protein. *Biochemistry*, **41**, 7998–8003.
 23. Rumbley, J., Hoang, L., Mayne, L. & Englander, S. W. (2001). An amino acid code for protein folding. *Proc. Natl Acad. Sci. USA*, **98**, 105–112.
 24. Wang, L. & Kallenbach, N. R. (1998). Proteolysis as a measure of the free energy difference between cytochrome *c* and its derivatives. *Protein Sci.* **7**, 2460–2464.
 25. Spolaore, B., Bermejo, R., Zambonin, M. & Fontana, A. (2001). Protein interactions leading to conformational changes monitored by limited proteolysis: Apo form and fragments of horse cytochrome *c*. *Biochemistry*, **40**, 9460–9468.
 26. Linderström-Lang, K. U. & Schellman, J. A. (1959). Protein structure and enzyme activity. In *The Enzymes* (Boyer, P. D., Lardy, H. & Myrback, K., eds), pp. 443–510, Academic Press, New York.
 27. Fetrow, J. S., Cardillo, T. S. & Sherman, F. (1989). Deletions and replacements of omega loops in yeast iso-1-cytochrome *c*. *Proteins: Struct. Funct. Genet.* **6**, 372–381.
 28. Fetrow, J. S., Dreher, U., Wiland, D. J., Schaak, D. L. & Boose, T. L. (1998). Mutagenesis of histidine-26 demonstrates the importance of loop-loop and loop-protein interactions for the function of iso-1-cytochrome *c*. *Protein Sci.* **7**, 994–1005.
 29. Garcia, A. E. & Hummer, G. (1999). Conformational dynamics of cytochrome *c*: correlation to hydrogen exchange. *Proteins: Struct. Funct. Genet.* **36**, 175–191.
 30. Fetrow, J. S. & Baxter, S. M. (1999). Assignment of ¹⁵N chemical shifts and ¹⁵N relaxation measurements for oxidized and reduced iso-1-cytochrome *c*. *Biochemistry*, **38**, 4480–4492.
 31. Baxter, S. M. & Fetrow, J. S. (1999). Hydrogen exchange behavior of [U-¹⁵N]-labeled oxidized and reduced iso-1-cytochrome *c*. *Biochemistry*, **38**, 4493–4503.
 32. Jemmerson, R., Liu, J., Hausauer, D., Lam, K.-P., Mondino, A. & Nelson, R. D. (1999). A conformational change in cytochrome *c* of apoptotic and necrotic cells is detected by monoclonal antibody binding and mimicked by association of the native antigen with synthetic phospholipid vesicles. *Biochemistry*, **38**, 3599–3609.
 33. Wallace, C. J. A. (1987). Functional consequences of the excision of an Ω loop, residues 40–55, from mitochondrial cytochrome *c*. *J. Biol. Chem.* **262**, 16767–16770.
 34. Wallace, C. J. A. (1993). Understanding cytochrome *c* function: engineering protein structure by semi-synthesis. *FASEB J.* **7**, 505–515.
 35. Westerhuis, L. W., Tesser, G. I. & Nivard, R. J. F. (1982). A functioning complex of two cytochrome *c* fragments with deletion of (39–58) eicosapeptide. *Int. J. Pept. Protein Res.* **19**, 290–299.
 36. Qin, W., Sanishvili, R., Plotkin, B., Schejter, A. & Margoliash, E. (1995). The role of histidines 26 and 33 in the structural stabilization of cytochrome *c*. *Biochim. Biophys. Acta*, **1252**, 87–94.
 37. Pettigrew, G. W. & Moore, G. R. (1987). *Cytochromes c*.

- Biological aspects. Springer Series in Molecular Biology* (Rich, A., ed.), Springer-Verlag, Berlin, Heidelberg, New York.
38. Kraulis, P. J. (1991). MOLSCRIPT: a program to produce both detailed and schematic plots of protein structures. *J. Appl. Crystallog.* **24**, 945–949.
39. Bai, Y., Milne, J. S., Mayne, L. & Englander, S. W. (1993). Primary structure effects on peptide group hydrogen exchange. *Proteins: Struct. Funct. Genet.* **17**, 75–86.
40. Connelly, G. P., Bai, Y., Jeng, M.-F. & Englander, S. W. (1993). Isotope effects in peptide group hydrogen exchange. *Proteins: Struct. Funct. Genet.* **17**, 87–92.

Edited by C. R. Matthews

(Received 29 April 2003; received in revised form 15 May 2003; accepted 27 May 2003)